APPLIED AND ENVIRONMENTAL MICROBIOLOGY, Aug. 1993, p. 2501–2510 Vol. 59, No. 8
0099-2240/93/082501-10$02.00/0

Kinetic Studies of Ammonia Monooxygenase Inhibition in *Nitrosomonas europaea* by Hydrocarbons and Halogenated Hydrocarbons in an Optimized Whole-Cell Assay

WILLIAM K. KEENER AND DANIEL J. ARP*

Laboratory for Nitrogen Fixation Research, Oregon State University, Corvallis, Oregon 97331-2902

Received 4 March 1993/Accepted 19 May 1993

The inhibitory effects of 15 hydrocarbons and halogenated hydrocarbons on NH_3 oxidation by ammonia monooxygenase (AMO) in intact cells of the nitrifying bacterium *Nitrosomonas europaea* were determined. Determination of AMO activity, measured as NO_2^- production, required coupling of hydroxylamine oxidoreductase (HAO) activity with NH_3-dependent NH_2OH production by AMO. Hydrazine, an alternate substrate for HAO, was added to the reaction mixtures as a source of reductant for AMO. Most inhibitors exhibited competitive or noncompetitive inhibition patterns. The competitive character generally decreased (K_{iE}/K_{iES} increased) as the molecular size of the inhibitors increased. For example, CH_4 and C_2H_4 were competitive inhibitors of NH_3 oxidation, whereas the remaining alkanes (up to C_4) and monohalogenated (Cl, Br, I) alkanes were noncompetitive. Oxidation of C_2H_5Br (noncompetitive) increased as the NH_4^+ concentration increased up to 40 mM, whereas oxidations of inhibitors with competitive character ($K_{iE} \ll K_{iES}$) were diminished at 40 mM NH_4^+. Multichlorinated compounds produced nonlinear Lineweaver-Burk plots. Iodinated alkanes (CH_3I, C_2H_5I) and C_2Cl_4 were potent inhibitors of NH_3 oxidation. Maximum rates of NH_3, C_2H_4, and C_2H_6 oxidations were approximately equivalent, suggesting a common rate-determining step. These data support an active-site model for AMO consisting of an NH_3-binding site and a second site that binds noncompetitive inhibitors, with oxidation occurring at either site.

The widely distributed soil bacterium *Nitrosomonas europaea* is an obligate chemolithoautotrophic aerobe which uses ammonia as its sole natural energy source (28). The oxidation of ammonia to nitrite in *N. europaea* is initiated by ammonia mono-oxygenase (AMO). Because of the broad substrate range of AMO (2, 19, 21, 24), attention has focused recently on the possibility of using nitrifiers such as *N. europaea* in the bioremediation of contaminated soils and aquifers and in the treatment of wastes. Exploitation of this potential of nitrifiers will require a thorough knowledge of AMO and its interaction with alternate substrates.

AMO catalyzes the oxidation of NH_3 to hydroxylamine which is subsequently oxidized to NO_2^- by hydroxylamine oxidoreductase (HAO) with the release of four electrons (28). Two of the four electrons must be transferred to AMO to activate O_2 and maintain steady-state rates of ammonia oxidation (28). Free NH_2OH concentrations are apparently very low during ammonia oxidation (28). The coupling of AMO and HAO activities is illustrated in the top half of Fig. 1. AMO in *N. europaea* also catalyzes the oxidation of several alternate substrates (including hydrocarbons and halogenated hydrocarbons) (19–21, 24). These oxidations, such as the oxidation of ethylene to ethylene oxide (Fig. 1, bottom half), require reductant, which can be supplied by the simultaneous oxidation of ammonia to provide NH_2OH.

Previous studies of halogenated hydrocarbon oxidations by *N. europaea* focused on the substrate range of the enzyme (11, 19–21, 24), product identification (11, 19), and the toxicity associated with the oxidation of some compounds (21, 24). As potential substrates for AMO, hydrocarbons and halogenated hydrocarbons can be categorized into three classes as defined by Rasche et al. (21): class 1 (those not oxidized by AMO), class 2 (those oxidized by AMO with little or no resultant toxic effect on the cells), and class 3 (those oxidized by AMO but yielding reactive products that inactivate NH_3 oxidation). Two examples of class 1 compounds are carbon tetrachloride and tetrachloroethylene (21). Chloromethane (21) and monohaloethanes (19) are class 2 substrates, which yield formaldehyde and acetaldehyde as oxidation products, respectively. Chloroform and trichloroethylene are examples of class 3 compounds, although both are oxidatively dechlorinated (21).

Although previous studies have provided information on the substrate range and other aspects of alternate substrate oxidations by AMO, they have provided little information on how halogenated hydrocarbon substrates interact with the active site of AMO. Kinetic inhibition studies can provide such insights into the active site of AMO and should therefore have predictive value for biotransformations of compounds structurally related to those we have tested, as well as for in situ biotransformations of mixtures of compounds. With whole cells of *N. europaea*, the inhibition of NH_3 oxidation by CH_4 (13) and C_2H_4 (14) is competitive, which indicates mutually exclusive binding of NH_3 and these alternate substrates. Benzene, which is oxidized to phenol and subsequently to *p*-hydroquinone, exhibits a noncompetitive pattern (12). At low NH_4^+ concentrations, the double-reciprocal plots for CH_4 and C_2H_4 deviate from the pattern expected for simple competitive inhibition; reductant depletion was cited as an explanation (14). Suzuki et al. (23) monitored AMO activity by measuring NH_3-dependent O_2 consumption in cell extracts and obtained double-reciprocal plots for the inhibitors CH_4, CO, and CH_3OH which are also indicative of competitive inhibition. Their plots also deviate somewhat from simple competitive inhibition.

* Corresponding author.

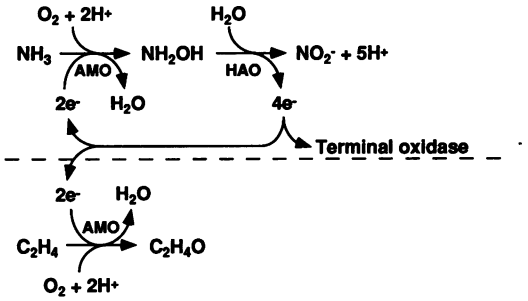

FIG. 1. Reactions catalyzed by AMO and HAO. Reactants are shown in numbers required for a single catalytic turnover event.

We wished to investigate the interactions of hydrocarbons and halogenated hydrocarbons with AMO by determining the inhibition patterns and apparent inhibition constants associated with the inhibition of NH_3 oxidation by these compounds. Since bioremediation applications with *N. europaea* would involve whole cells, our experiments were carried out with intact cells. Active, purified preparations of AMO are not available. Furthermore, there is considerable difficulty involved in stabilizing and assaying cell extracts (6). The direct electron donor for AMO has not been identified, necessitating the use of a coupled enzyme system, as in our study. The efficiency of coupling of AMO and HAO activities is apparently greatly reduced when cells are lysed (6). Alternate substrates can influence AMO activity in intact cells by three distinct mechanisms: (i) direct binding and interaction with AMO, (ii) interference with the reductant supply to AMO (oxidation of alternate substrates requires reductant, but the products are not further oxidized to replenish the reductant as is the case with NH_3), or (iii) oxidation to highly reactive products that covalently bind and inactivate AMO and other enzymes. To avoid the cytotoxic effects associated with reactive products, we limited our study to class 1 and 2 compounds. To ensure a constant supply of reductant to AMO, we included hydrazine, an alternate substrate for HAO, in the reaction mixtures. In this way, we attempted to restrict the inhibitory effects of class 2 compounds to direct interactions with AMO. Fifteen hydrocarbon and halogenated hydrocarbon inhibitors produced a variety of inhibition patterns including competitive, noncompetitive, and nonlinear (concave-down) v^{-1}-versus-S^{-1} plots (for definitions of v and S, see Materials and Methods). Within the selection of inhibitors, trends were noted in molecular size, identity of the halogen substituent, and number of halogen substituents. These trends should enhance the predictive value of the present work.

MATERIALS AND METHODS

Cell growth and preparation. *N. europaea* ATCC 19718 was cultured in 1.5-liter batches at 30°C. The growth medium contained 25 mM $(NH_4)_2SO_4$ and other constituents as described previously (21). Cultures were inoculated with 40 ml of a 2-day-old culture of *N. europaea* grown on the same medium. Nitrite concentrations were determined spectrophotometrically by using the formula $(A_{352} - A_{400})/0.0225 = [NO_2^-]$ (millimolar concentration). When the NO_2^- concentrations in the medium reached 15 to 21 mM (~42 h), the cells were harvested by centrifugation. At this age, the cell culture is in the late exponential growth phase; AMO activity for a given cell density is maximal (9) and consistent (as indicated by the day-to-day consistency of V_{max} and K_m values for control curves in v^{-1}-versus-S^{-1} plots [see below]. The cells were washed once in assay buffer, consisting of 50 mM NaH_2PO_4 (pH 7.7) and 2 mM $MgCl_2$, and then sedimented and resuspended in assay buffer to a constant cell density (1.8 mg of protein per ml). Cell suspensions were prepared daily, stored on ice in the dark, and used within 15 h. Protein content was determined by using the biuret assay (7) after the cells were solubilized in 3 N NaOH for 1 h at 65°C.

Materials. Liquid inhibitors included CCl_4 (Fisher, Fair Lawn, N.J.); C_2H_5Cl (Kodak, Rochester, N.Y.); and C_2H_5Br, C_2Cl_4, C_2H_5I, CH_3I, CCl_3CH_2Cl, and n-ClC_3H_7 (Aldrich Chemical Co., Milwaukee, Wis.). Gaseous inhibitors included CH_4 and C_2H_4 (Airco, Vancouver, Wash.); C_3H_8 and n-C_4H_{10} (Aldrich); and CH_3Br, CH_3Cl, and C_2H_6 (Liquid Carbonic, Chicago, Ill.). The purities of all compounds were ≥99% unless otherwise noted. Other reagents included 1-allyl-2-thiourea (Kodak), $NH_2OH \cdot HCl$ (97.8% pure; Fisher), $N_2H_4 \cdot H_2SO_4$ (Fisher), and $(NH_4)_2SO_4$ (Mallinckrodt, Paris, Ky.). All other chemicals were of reagent grade.

Kinetic inhibition assays. Stock solutions of the liquid inhibitors were prepared by adding the compounds to buffer-filled vials with microsyringes. Solutions were stirred magnetically to achieve equilibrium, and then appropriate volumes were added with microsyringes to glass serum vials (volume, 6.5 ml) sealed with butyl rubber stoppers (Teflon-lined stoppers were used with C_2Cl_4). Gaseous inhibitors were added directly to sealed serum vials with microsyringes. Serum vials contained 4.9 ml of assay buffer. Inhibitor concentrations in the liquid phase of the assay vials were calculated from dilutions (solutions of liquids in buffer) or volumes added (gases), accounting for partitioning between the gas and liquid phases (determined by gas chromatography). Cells (50 μl of the aforementioned suspension) were added to the reaction vials, which were preincubated for 10 min in a water bath with shaking at 30°C. The reactions were initiated by addition of an aqueous solution (50 μl) containing $(NH_4)_2SO_4$ and N_2H_4 in concentrations appropriate to give the desired initial concentrations in the assay vials. The vials were shaken in a reciprocating water bath (three reciprocations per s) at 30°C. After 10 min, the reactions were stopped by addition of 1-allyl-2-thiourea (to 40 μM), a potent, specific inhibitor of NH_3 oxidation (16). The amount of NO_2^- produced in the reactions was determined colorimetrically (8). For the experiment whose results are shown in Table 1, NH_3 concentrations were determined colorimetrically as described previously (27).

To examine NH_3 as an inhibitor of C_2H_4 oxidation by AMO, we determined the inhibition pattern for several fixed NH_4^+ concentrations with variable C_2H_4 concentrations. The production of ethylene oxide was quantified by gas chromatography as described previously (19) (see Fig. 5). The reaction conditions were as described above, including the addition of an optimized concentration of N_2H_4 for each combination of NH_4^+ and C_2H_4 (see below).

Analysis of kinetic inhibition data. The rates of NO_2^- formation (v) (or of C_2H_4O formation [see Fig. 5]) obtained at various NH_4^+ concentrations (S) at a fixed inhibitor concentration were fit to the equation $v = (V_{max} \cdot S)(K_m + S)^{-1}$ by using the unweighted least-squares method and the Marquardt-Levenberg algorithm for nonlinear curve fitting (SigmaPlot; Jandel Corp.). Data for tetrachlorinated inhibitors clearly exhibited more complex behavior than for the remaining inhibitors; therefore, K_i values were not deter-

mined for these compounds. The datum points in Fig. 7 are connected by straight lines to indicate that they correspond to a given inhibitor concentration. The kinetic inhibition data were plotted as v^{-1} versus S^{-1} at several inhibitor concentrations to facilitate visual analysis. The inhibition constants K_{iE} and K_{iES} were obtained by replotting the inhibitor concentrations versus the slopes or y intercepts obtained on the v^{-1}-versus-S^{-1} plots, respectively. The constants were taken as the absolute values of the x intercepts on the appropriate replots. For purified enzymes with one substrate and an unreactive inhibitor, K_{iE} and K_{iES} are the dissociation constants for binding of the inhibitor to the free enzyme (E) and the enzyme-substrate complex (ES), respectively (4). Our system provides apparent K_i values that cannot be considered true dissociation constants. However, these values should provide reasonable approximations for the relative affinities of these inhibitors for AMO in vivo.

Addition of hydrazine to circumvent reductant limitation. To eliminate reductant depletion caused by the oxidation of alternate substrates by AMO, we added hydrazine to the reaction mixture at a concentration that gave the maximum NO_2^- production rate. This optimum N_2H_4 concentration was determined empirically for each combination of NH_4^+ and inhibitor concentrations as follows. Hydrazine concentrations (0, 0.1, 0.2, 0.3, 0.5, 0.7, and 0.9 mM) were tested for 0.5, 1, and 5 mM NH_4^+ for each of the high, low, and intermediate inhibitor concentrations (five concentrations were used for most inhibitors). The optimum N_2H_4 concentration was then interpolated for the remaining combinations of NH_4^+ and inhibitor concentrations.

V_{max} and K_m determinations for C_2H_4 and C_2H_6. V_{max} and K_m values were determined for the alternate substrates C_2H_4 and C_2H_6 by using N_2H_4 (added from aqueous stock solutions) to provide reductant. Oxidation rates of C_2H_4 and C_2H_6 were maximized with 0.8 mM N_2H_4; varying the N_2H_4 concentration was unnecessary. The respective products ethylene oxide and ethanol were quantified by gas chromatography as described previously (19). All other reaction conditions were as described above.

Alternate substrate oxidations with NH_3 as the sole reductant source. The effects of increasing NH_4^+ concentrations on the oxidation rates of C_2H_4, CH_3Br, C_2H_5Br, and CH_3Cl were determined. The alternate substrates (300 μM in the aqueous phase) were combined with cells, preincubated as above, and $(NH_4)_2SO_4$ was added (final NH_4^+ concentrations, 1, 2, 5, 10, 20, and 40 mM) to initiate the reaction. Oxidation rates with endogenous reductant only were determined in the absence of NH_4^+ (see Table 4). Hydrocarbon and halogenated hydrocarbon oxidations were determined as the amount of product formed or the difference between the initial substrate concentrations and the substrate concentration that remained after a fixed period. Substrates and products were quantified with liquid-phase injections by using gas chromatography. All other reaction conditions were as described above.

RESULTS

Determination of the validity of a coupled assay to measure rates of NH_3 oxidation in the presence of AMO inhibitors. We sought to investigate the kinetic mechanisms of the interactions of hydrocarbon and halogenated hydrocarbon compounds with the physiological substrate NH_3. AMO activity can be determined in a number of ways, including gas-chromatographic analysis of organic substrate depletion and determination of the residual NH_4^+ concentration by use of an ion-selective electrode or a colorimetric assay. However, these methods suffer from the need to accurately determine small changes in NH_3 or alternate substrate concentration. We chose to determine rates of NO_2^- production from NH_3 as a measure of AMO activity; colorimetric NO_2^- quantification is a simple and sensitive assay. A shortcoming of this method is that NO_2^- production involves the coupling of two enzyme activities—AMO and HAO—through the intermediate NH_2OH. Therefore, a number of assumptions are inherent in this assay. The first assumption was that all the oxidized NH_3 was converted to NO_2^-. To test this assumption, we performed an experiment in which the amounts of NH_3 consumed were determined and compared with the amounts of NO_2^- produced under various experimental conditions. As shown in Table 1, the amount of NH_3 consumed after incubation for 1 h equaled the amount of NO_2^- produced under all conditions tested, which included the presence of a representative inhibitor, C_2H_4 (690 μM), and/or the reductant N_2H_4 (0.7 mM). This approach was not feasible for measuring small changes in NH_4^+ concentration occurring during 10-min reaction periods, as used in the kinetic assays. However, when the highest concentration of an alternate substrate/inhibitor was used (with its optimal N_2H_4 concentration [see below]) and AMO was specifically and rapidly inactivated with C_2H_2 after 10-min reactions, no significant further increases in NO_2^- concentration were measured after continued incubation of the reaction mixtures. Supraoptimal N_2H_4 concentrations diminished NO_2^- production over 10-min reactions but also correlated with significant increases in NO_2^- concentration with extended incubations. These observations can be explained if negligible NH_2OH concentrations accumulate with optimal N_2H_4 concentrations, whereas supraoptimal N_2H_4 concentrations cause accumulation of NH_2OH.

TABLE 1. Comparison of ammonium consumed and nitrite produced by whole cells of *N. europaea* in the presence of ethylene and/or hydrazine[a]

Addition	Amt of ammonium consumed (μmol)	Amt of nitrite produced (μmol)
0.5 mM NH_4^+	1.52	1.58
1 mM NH_4^+	2.76	2.77
0.5 mM NH_4^+ + 0.7 mM N_2H_4	1.18	1.19
1 mM NH_4^+ + 0.7 mM N_2H_4	1.93	1.89
0.5 mM NH_4^+ + 690 μM C_2H_4 + 0.5 mM N_2H_4	0.61	0.61
1 mM NH_4^+ + 690 μM C_2H_4 + 0.5 mM N_2H_4	1.14	1.16

[a] Reactions were stopped with C_2H_2 after 1 h. Ammonium and nitrite concentrations were measured as described in Materials and Methods.

The second assumption was that changes in the concentrations of substrates, inhibitors, and products during the time course of the reaction (10 min) did not affect the observed rates of NO_2^- production. To test this assumption, we determined time courses of NO_2^- production with the inhibitor C_2H_4 under the conditions used for Fig. 2. The reaction rates were constant up to 16 min. In subsequent experiments, the rates were determined from the first 10 min of the reaction. Similar tests of rate constancy were conducted for all 15 compounds examined; rates of NO_2^- production were constant over the time course of the experiments, with only C_2H_5Br and C_2H_5I causing slight rate decreases at the highest inhibitor concentrations.

The third assumption was that any inhibition of NH_3

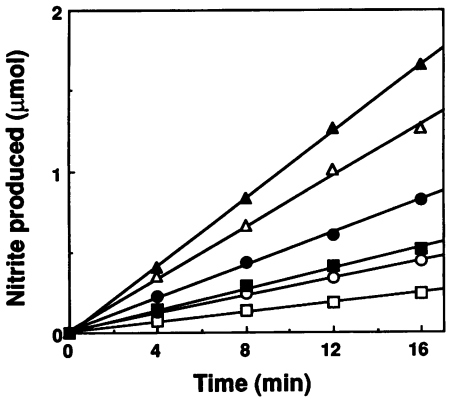

FIG. 2. Time courses of NO_2^- production by *N. europaea*. For each line, reactions in quintuplicate vials were initiated by addition of cells and individually stopped at 4-min intervals by addition of C_2H_2. For vials containing C_2H_4, N_2H_4 concentrations providing maximum NO_2^- production were determined (see Materials and Methods) and included in quintuplicate vials. Symbols: ■, 0.5 mM NH_4^+; ●, 1 mM NH_4^+; ▲, 5 mM NH_4^+; □, 0.5 mM NH_4^+ + 690 μM C_2H_4 + 0.7 mM N_2H_4; ○, 1 mM NH_4^+ + 690 μM C_2H_4 + 0.7 mM N_2H_4; △, 5 mM NH_4^+ + 690 μM C_2H_4 + 0.3 mM N_2H_4.

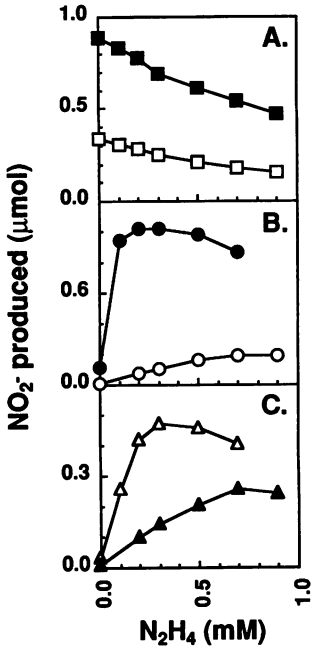

FIG. 3. Influence of N_2H_4 on NO_2^- production by *N. europaea*. (A) Inhibition of NH_4^+-dependent NO_2^- production by N_2H_4 in the absence of an alternate substrate. Reactions were stopped by addition of aliquot to acidic NO_2^- assay reagent immediately after a 10-min reaction. Symbols: □, 0.5 mM NH_4^+; ■, 5 mM NH_4^+. (B) Influence of NH_4^+ on the optimum N_2H_4 concentration required for maximum NO_2^- production with 690 μM C_2H_4 present. Symbols: ○, 0.5 mM NH_4^+; ●, 5 mM NH_4^+. (C) Influence of C_2H_4 on the optimum N_2H_4 concentration required for maximum NO_2^- production from 1 mM NH_4^+. Symbols: △, 170 μM C_2H_4; ▲, 1,040 μM C_2H_4.

oxidation observed was specific for AMO and was not due to inhibition of HAO or other enzymes involved in the coupled reaction. To test this assumption, we investigated whether the oxidation of NH_2OH to NO_2^- by HAO was influenced by any of the 15 inhibitors tested. AMO was inactivated with C_2H_2, a mechanism-based inactivator of AMO (15). Reactions were stopped after 8 min by addition of an aliquot of the reaction mixture to the acidic reagent for the NO_2^- assay. Even at the highest concentrations of the inhibitors used to obtain the kinetic data, the oxidation of NH_2OH (200 μM) was not inhibited by 14 of the compounds. Only CCl_3CH_2Cl (1.2 mM) inhibited the oxidation of NH_2OH (by 18%). This indicates that HAO and other enzymes and proteins required in the oxidation of NH_2OH to NO_2^- in intact cells were not influenced by the inhibitors.

Because the reactions were carried out with intact cells, a fourth assumption was that NH_4^+ diffusion gradients between the medium and the cell periplasm were not influenced by changes in AMO activity. To determine whether NH_4^+ concentration gradients exist, we partially and specifically inactivated AMO in whole cells with light (10) and then adjusted the concentration of the cells to give the same maximum velocity of NO_2^- production as in untreated control cells (at 20 mM NH_4^+). Rates of NO_2^- production as a function of NH_4^+ concentration (0.33 to 20 mM) were determined. AMO inactivation should allow any NH_4^+ diffusion gradient to approach equilibrium, resulting in a decrease in the apparent K_m for NH_4^+ (17). With 0, 52, 82, and 92% inactivation, the apparent K_ms were 1.21, 1.17, 1.11, and 1.02 mM, respectively. These results suggest that an NH_4^+ diffusion gradient, if it existed, was small. Therefore, any changes in the gradient as a result of addition of inhibitors would not be expected to have a significant impact on the kinetics of NO_2^- production. In summary, these results confirm the validity of determining rates of NO_2^- production from intact cells as a measure of AMO activity.

Addition of hydrazine to circumvent reductant limitation. In previous studies, it was shown that the effects of alternate substrates on the rates of AMO activity cannot be accounted for solely by direct effects occurring at the active site of AMO (14, 19). Because the products of the alternate-substrate oxidations are not further oxidized, the oxidation of alternate substrates by AMO results in a net drain of reductant (Fig. 1). To discriminate between direct NH_3 and inhibitor interactions on AMO and any secondary effects due to reductant limitation, it was necessary to eliminate the latter effects. This was achieved by addition of hydrazine to the reaction mixtures. Hydrazine is an alternate substrate for HAO (18), is an effective electron donor for AMO-catalyzed oxidations (13), and is oxidized by HAO to produce N_2, which does not interfere with the colorimetric NO_2^- assay.

Addition of N_2H_4 to cells in the presence of NH_4^+ and the absence of a hydrocarbon inhibitor did not stimulate the rates of NO_2^- production, indicating that NH_3 oxidation was not reductant limited under such conditions. Indeed, increasing concentrations of N_2H_4 progressively inhibited the rates of NO_2^- production (Fig. 3A). Excess N_2H_4 might prevent the oxidation of NH_2OH generated from NH_3 and hence decrease the amount of NO_2^- detected. Furthermore, the subsequent increase in the intracellular concentration of NH_2OH may lead to direct inhibition of AMO (1, 14). It seems unlikely that N_2H_4 directly inhibited AMO activity at the concentrations used (<1 mM) in the inhibition experiments, because, in the absence of NH_4^+, the rate of ethylene (920 μM) oxidation was not diminished at 1.0 mM N_2H_4 relative to lower concentrations (data not shown).

The effects of N_2H_4 addition on the rates of NO_2^- production in the presence of the inhibitor C_2H_4 are shown

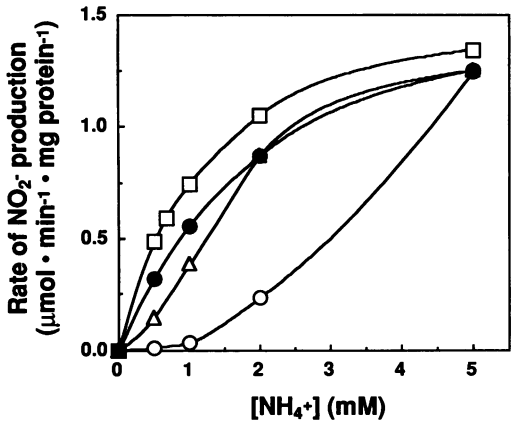

FIG. 4. Effect of N_2H_4 on NH_4^+-dependent NO_2^- production rates by *N. europaea* in the presence of 345 μM C_2H_4 (and control). Symbols: □, NH_4^+ only; ○, C_2H_4 without N_2H_4; △, C_2H_4 + 0.1 mM N_2H_4; ●, N_2H_4 concentrations selected (for each NH_4^+ concentration) which yielded maximum NO_2^- production.

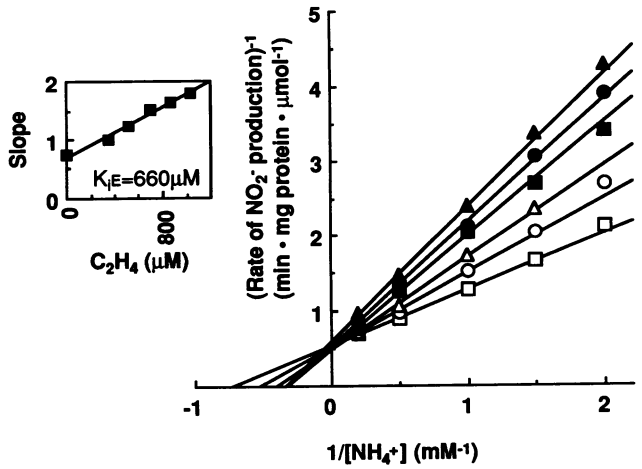

FIG. 5. Lineweaver-Burk plot for C_2H_4 as an inhibitor of NH_4^+-dependent NO_2^- production in *N. europaea*. Symbols: □, 0 μM C_2H_4; ○, 345 μM C_2H_4; △, 520 μM C_2H_4; ■, 690 μM C_2H_4; ●, 860 μM C_2H_4; ▲, 1,040 μM C_2H_4. (Inset) Slope replot. Slopes of curves were plotted against inhibitor concentration to obtain K_{iE}, the absolute value of the x intercept.

in Fig. 3B and C. In contrast to the situation in the absence of C_2H_4, low concentrations of N_2H_4 stimulated the rate of NO_2^- production in the presence of C_2H_4. This stimulation was attributed to circumvention of the reductant limitation imposed by the oxidation of C_2H_4. As in the absence of an alternate substrate, higher concentrations of N_2H_4 resulted in a decreased rate of NO_2^- production, presumably for the reasons stated above. These results demonstrate that different concentrations of N_2H_4 are required to achieve optimal rates of NO_2^- formation under different conditions. Since increasing concentrations of the same compound will cause greater depletion of the reductant supply (Fig. 3C), it is obvious that each set of experimental conditions is associated with a unique optimal N_2H_4 concentration. Therefore, in all subsequent experiments, the concentration of N_2H_4 supporting the maximum rate of NO_2^- production was determined for each unique set of conditions. Throughout this text, "optimal N_2H_4 concentration" refers to the concentration of N_2H_4 required to maximize the rate of NO_2^- production under the stated conditions.

Maximum NO_2^- production rates with optimal N_2H_4 concentrations were constant for 16 min (Fig. 2). Also, NH_3-dependent NO_2^- production equaled NH_3 consumption over 1 h when 0.7 mM N_2H_4 was present (Table 1). These results show that the assumptions of the previous section were still valid when N_2H_4 was included in the assay. We also assumed that optimal N_2H_4 concentrations replenished the reductant to a constant level and that only the initial inhibitor and NH_3 concentrations varied significantly among reaction vials.

Saturation kinetics are observed in the coupled assay. The coupled assay (NH_3 to NO_2^-), with addition of optimized concentrations of N_2H_4, was used to determine the velocity of NH_3 oxidation as a function of NH_3 concentration. As shown in Fig. 4, saturation kinetics were observed for NH_3 alone. When C_2H_4 was included in the reaction mixture, the rates of NO_2^- production decreased and the pattern was no longer typical of saturation kinetics. Addition of a single concentration of N_2H_4 (0.1 mM) increased the rates, but the curve was not hyperbolic. However, when optimized concentrations of N_2H_4 were added to the reaction mixture along with C_2H_4, the plot once again was typical of saturation kinetics, albeit with an apparently higher K_m. Thus, including optimal N_2H_4 concentrations was necessary to obtain saturation kinetics.

Kinetic inhibition patterns and constants. By using the assay described above, we investigated the inhibition of NH_3 oxidation to NO_2^- by the 15 hydrocarbons and halogenated hydrocarbons listed above. Except for CH_3I, all of these inhibitors have been reported to be either substrates for AMO or class 1 nonsubstrates (C_2Cl_4 and CCl_4) (11, 20, 21). For each inhibitor, a series of v^{-1}-versus-S^{-1} curves were obtained, with each curve representing a fixed concentration of inhibitor. Because each experiment included a control saturation curve with no inhibitor added, this provided a means of determining the day-to-day variability of the kinetic data. In 15 experiments, an average K_m for NH_4^+ of 1.34 ± 0.22 mM and an average V_{max} of 1.59 ± 0.17 μmol · min^{-1} · mg of $protein^{-1}$ were determined. This consistency facilitated comparison of results obtained on different days.

As an example of this approach, the results of the inhibition of NH_3 oxidation by C_2H_4 are shown in Fig. 5. The double-reciprocal plot reveals a pattern typical of a competitive inhibitor. The replot of slopes versus inhibitor concentrations (slope replot) is linear and yields a K_{iE} of 660 μM (Fig. 5 inset). We also determined the inhibition pattern with NH_3 as the inhibitor and C_2H_4 as the variable substrate. The rate of ethylene oxide formation was determined. Again, the pattern was typical of a competitive inhibitor, although the slope replot was not linear (Fig. 6). For a competitive inhibitor which also acts as a substrate, the K_i for the compound as inhibitor should equal its K_m as substrate (4). The K_i for C_2H_4 of 660 μM compares favorably with the K_m for C_2H_4 of 658 ± 154 μM (see Table 3). Methane was also a competitive inhibitor of NH_3 oxidation (see Table 2). The K_i for CH_4 (3,240 μM) was about fivefold higher than the K_i for C_2H_4. The high K_i for CH_4 is consistent with the observation that CH_4 is a relatively poor substrate for AMO (13).

Most of the compounds we examined did not give inhibition patterns typical of competitive inhibitors. Indeed, non-

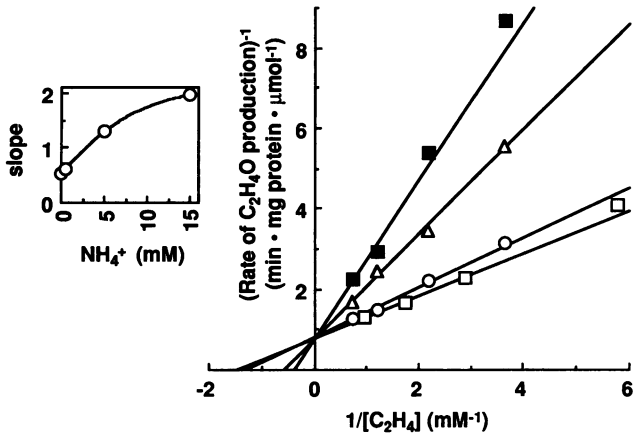

FIG. 6. Lineweaver-Burk plot for NH_3 as an inhibitor of C_2H_4 oxidation by *N. europaea*. Ethylene oxide production as a function of C_2H_4 concentration. Symbols: □, 0 mM NH_4^+; ○, 0.5 mM NH_4^+; △, 5 mM NH_4^+; ■, 15 mM NH_4^+. (Inset) Slope replot.

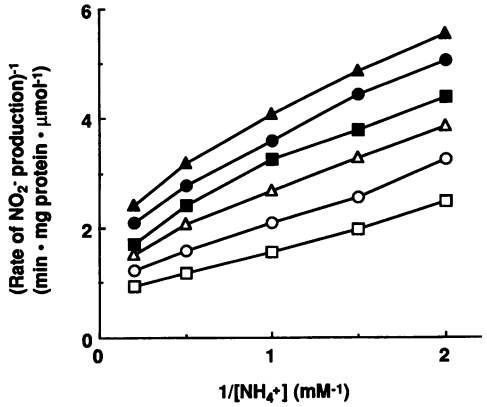

FIG. 8. Lineweaver-Burk plot for CCl_4 as an inhibitor of NH_4^+-dependent NO_2^- production in *N. europaea*. Symbols: □, 0 μM CCl_4; ○, 75 μM CCl_4; △, 150 μM CCl_4; ■, 225 μM CCl_4; ●, 300 μM CCl_4; ▲, 375 μM CCl_4.

competitive patterns were the most common. The double-reciprocal plot obtained for C_2H_5Cl (Fig. 7) exemplifies the noncompetitive pattern for inhibition of NH_3 oxidation. Replots (Fig. 7 inset) of inhibitor concentrations versus slopes or *y* intercepts of the curves in Fig. 7 provided values for K_{iE} (1.41 mM) and K_{iES} (1.42 mM), respectively. These similar values may have resulted from C_2H_5Cl having equal affinity to free enzyme (E) and to the ES complex (i.e., enzyme with NH_3 bound). All other noncompetitive inhibitors exhibited mixed noncompetitive patterns ($K_{iE} \neq K_{iES}$). These inhibitors were the hydrocarbons C_2H_6, C_3H_8, and n-C_4H_{10} and the halogenated hydrocarbons CH_3Cl, n-ClC_3H_7, CH_3Br, C_2H_5Br, CH_3I, and C_2H_5I. The iodinated compounds gave the lowest K_{iE} and K_{iES} values, which indicates strong binding to AMO. Ratios of K_{iE}/K_{iES} increased in the following sequence: CH_3Cl (0.20), C_2H_6 (0.25), CH_3Br (0.33), C_2H_5Cl (0.99), C_2H_5Br (2.23), n-C_4H_{10} (3.07), C_3H_8 (3.25), CH_3I (4.33), n-ClC_3H_7 (5.10), and C_2H_5I (9.67). With the inhibitors propylene, *trans*-dichloroethylene, CH_2ClCH_2Cl, and CH_2BrCH_2Cl, the rates of NH_3 oxidation as a function of time were constant only at inhibitor concentrations causing little inhibition of NH_3 oxidation. Nonetheless, all four inhibitors showed noncompetitive patterns at these low concentrations (data not shown).

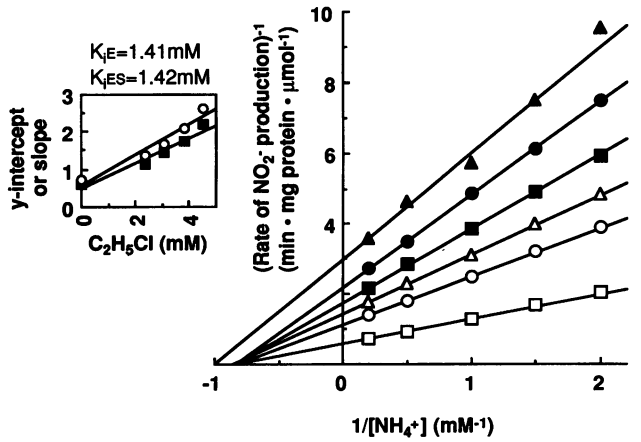

FIG. 7. Lineweaver-Burk plot for C_2H_5Cl as an inhibitor of NH_4^+-dependent NO_2^- production in *N. europaea*. Symbols: □, 0 mM C_2H_5Cl; ○, 2.34 mM C_2H_5Cl; △, 3.07 mM C_2H_5Cl; ■, 3.80 mM C_2H_5Cl; ●, 4.54 mM C_2H_5Cl; ▲, 5.27 mM C_2H_5Cl. (Inset) Slope and intercept replots. The inhibitor concentration was replotted against slopes (○) or *y* intercepts (■) to obtain K_{iE} and K_{iES}, respectively. Data from the 5.27 mM C_2H_5Cl curve were omitted from replots.

Not all compounds gave inhibition patterns typical of either competitive or noncompetitive inhibitors. With the tetrachlorinated compounds C_2Cl_4, CCl_4, and CCl_3CH_2Cl, the double-reciprocal plots were nonlinear. For example, the plot for CCl_4 (Fig. 8) shows concave-down curves, especially at high inhibitor concentrations. This pattern does not allow determination of K_{iE} and K_{iES} values. For comparison with other inhibitors, Table 2 includes inhibitor concentrations causing 50% inhibition of NO_2^- production from 1 mM NH_4^+. By this measure, C_2Cl_4 was the most potent inhibitor we examined.

For each inhibitor we investigated, the range of N_2H_4 concentrations required to optimize the rates of NO_2^- production is indicated in Table 2. For example, with C_2H_4 the optimal N_2H_4 concentrations varied from 0.1 to 0.7 mM and N_2H_4 requirements were influenced by the NH_4^+ concentration (Fig. 3B). In general, the higher C_2H_4 concentrations required higher N_2H_4 concentrations to replace the reductant diverted to C_2H_4 oxidation (Fig. 3C). Other inhibitors previously shown to be oxidized rapidly (19) also required high concentrations of N_2H_4 to replenish reductant and maximize NO_2^- production, whereas slowly oxidized inhibitors required lower concentrations of N_2H_4 (19, 21). For inhibitors with competitive character, (K_{iE}/K_{iES} ratios, <1), the optimal N_2H_4 concentration decreased with increasing NH_4^+ concentration. This is consistent with a decreased diversion of reductant to the alternate substrate as its binding to AMO was outcompeted by NH_3; NH_3-derived NH_2OH would provide more of the total reductant at higher NH_4^+ concentrations. For noncompetitive oxidizable inhibitors with $K_{iE}/K_{iES} \geq 1$ (including C_2H_5Cl), the optimal N_2H_4 requirements increased with increasing inhibitor concentration but did not vary with the NH_4^+ concentration for a given inhibitor concentration. In contrast, compounds that were oxidized only slowly (such as CH_3I, C_2H_5I, or CCl_3CH_2Cl) (19, 21) or not at all (C_2Cl_4 and CCl_4) (21)

TABLE 2. Apparent kinetic inhibition constants from slope and intercept replots of v^{-1} versus S^{-1} plots with *N. europaea* whole cells

Inhibitor	Inhibition pattern[a]	K_{iE} (μM)[b]	K_{iES} (μM)[b]	$[\mu M\ I]_{50\%}$ (1 mM NH_4^+)[c]	$[N_2H_4]$ range used (mM)[d]	K_{iE}/K_{iES}
Methane	C	3,240		>1,800	0.05–0.3	
Ethane	NC	220	890[e]	520	0.1–0.5	0.25
Propane	NC	1,430	440	840	0.1–0.5	3.25
n-Butane	NC	920	300	450	0.2–0.5	3.07
Ethylene	C	660		550	0.1–0.7	
Chloromethane	NC	300	1,470	550	0.1–0.7	0.20
Chloroethane	NC	1,410[e]	1,420[e]	2,340	0.3–0.7	0.99
n-Chloropropane	NC	5,150[e]	1,010	2,000	0.3–0.5	5.10
Bromomethane	NC	500	1,490	770	0.1–0.7	0.33
Bromoethane	NC	490	220	550	0.1–0.7	2.23
Iodomethane	NC	130	30	80	0	4.33
Iodoethane	NC	290	30	80	0.1	9.67
Tetrachloroethylene	CD			5	0	
Carbon tetrachloride	CD			300	0	
1,1,1,2-Tetrachloroethane	CD			500	0.1	

[a] Patterns of curves on double-reciprocal plots were as follows: C, competitive; NC, noncompetitive; CD, concave-down.

[b] K_{iE} and K_{iES} are apparent inhibition constants derived from slope and intercept replots, respectively. Data in replots were fit to the $y = mx + b$ formula by the least-squares method.

[c] These values represent the micromolar inhibitor concentrations required for 50% inhibition of NO_2^- production from 1 mM NH_4^+. The N_2H_4 concentration was optimized in each case.

[d] These values include the N_2H_4 concentrations used in the kinetic assays.

[e] One (C_2H_5Cl and C_2H_6) or two (*n*-ClC_3H_7) datum points were omitted from these replots. The remaining replots included all (five or six) datum points. r^2 values for all slope replots exceeded 0.91 (average, 0.97 ± 0.03). Except for *n*-C_4H_{10} ($r^2 = 0.89$), r^2 values for intercept replots exceeded 0.95 (average, 0.97 ± 0.03).

required little (0.1 mM) or no N_2H_4 to supplement NH_3-derived reductant.

V_{max} values were obtained for the oxidation of C_2H_6 to ethanol and of C_2H_4 to ethylene oxide in the presence of N_2H_4 and the absence of competing NH_3. In Table 3 the values are compared with those obtained for NH_3. All three V_{max} values are about 1.5 μmol · min^{-1} · mg of $protein^{-1}$. The K_m values for C_2H_4 and C_2H_6 are similar and are lower than the value obtained for NH_4^+. However, the substrate for AMO is considered to be NH_3, not NH_4^+ (3). At pH 7.7, 1.35 mM NH_4^+ corresponds to an NH_3 concentration of 54 μM. Thus, the K_m for NH_3 is about 10-fold lower than the K_ms for C_2H_4 and C_2H_6. In these experiments, 0.8 mM N_2H_4 did not inhibit the oxidation of C_2H_4 and C_2H_6 at their lowest concentrations and was adequate for their highest concentrations; therefore, 0.8 mM N_2H_4 was used at all substrate concentrations.

Alternate substrate oxidations with NH_3 as the sole reductant source. The effects of increasing the concentration of NH_4^+ on the oxidations of alternate substrates were studied to corroborate the inhibition data by further characterizing the interactions of NH_3 with alternate substrate inhibitors. High concentrations of NH_3 (>10 mM) were found to inhibit the oxidation of C_2H_4 (Table 4), with maximum C_2H_4O production occurring at 5 mM NH_4^+. Oxidation of C_2H_5Br, a clearly noncompetitive inhibitor ($K_{iE} > K_{iES}$), was not diminished at high NH_4^+ concentrations; 40 mM NH_4^+ caused the greatest acetaldehyde production (0.44 μmol in 10 min). However, some noncompetitive inhibitors showed competitive character ($K_{iE} \ll K_{iES}$); CH_3Cl and CH_3Br were chosen as examples. Substrate depletion was used to monitor their oxidation; maximum substrate depletion occurred with 2 mM NH_4^+ for CH_3Cl and with 5 mM NH_4^+ for CH_3Br. These results are comparable to those for C_2H_4.

DISCUSSION

We studied the inhibition by hydrocarbons and halogenated hydrocarbons of NH_3 oxidation by AMO to learn more about the interaction of these compounds with this enzyme. Despite the complexity of the experimental system, NO_2^- production rates at various NH_3 and inhibitor concentrations yielded inhibition plots showing simple patterns. The patterns we observed can be interpreted in terms of direct inhibitor binding to the enzyme. We observed a variety of inhibition patterns ranging from competitive to nearly uncompetitive, as well as some nonclassical inhibition patterns. Our data suggest that some inhibitors bind predominantly to the site on AMO which also binds NH_3, whereas other inhibitors are not excluded when NH_3 is bound to the enzyme. We propose an active-site model for AMO which consists of an NH_3-binding site to which competitive inhibitors bind and an alternate site to which noncompetitive inhibitors bind. Additional binding sites would be required for O_2 and the site of electron donation.

Because CH_4 and C_2H_4 competitively inhibit NH_3 oxidation, it seems reasonable that these compounds bind predominantly to the same specific site to which NH_3 binds. That C_2H_4 and NH_3 bind to the same site is further evidenced by the observation that the K_{iE} (Table 2) and K_m

TABLE 3. Apparent kinetic parameters from reaction rate studies with *N. europaea*

Substrate	Mean V_{max} ± SD[a] (μmol of product/min/mg of protein)	Mean K_m ± SD[a] (μM)	No. of trials
Ammonium	1.68 ± 0.15	1,353 ± 109	3
Ethylene	1.56 ± 0.23	658 ± 154	4
Ethane	1.44 ± 0.08	522 ± 27	2

[a] SD, standard deviation.

TABLE 4. Extents of alternate substrate oxidations by *N. europaea* cells with increasing NH_4^+ concentrations[a]

NH_4^+ concn (mM)	Amt of C_2H_4O produced from C_2H_4 (μmol)	Amt of CH_3CHO produced from C_2H_5Br (μmol)	Amt of CH_3Br consumed (μmol)	Amt of CH_3Cl consumed (μmol)
0	0	0	0.144	0.007
1	0.031	0.054	0.411	0.261
2	0.184	0.062	0.421	0.438
5	0.194	0.224	0.433	0.327
10	0.134	0.251	0.357	0.301
20	0.095	0.293	0.306	0.299
40	0.077	0.444	0.229	0.257

[a] All initial substrate concentrations in liquid medium were 300 μM. Reaction times for oxidations of C_2H_4, C_2H_5Br, CH_3Br, and CH_3Cl were 10, 10, 25, and 30 min, respectively.

(Table 3) values for C_2H_4 are both 660 μM. This result is predicted for competing substrates, one of which is treated as the inhibitor (4). Conversely, Fig. 6 shows that NH_3 is a competitive inhibitor of C_2H_4 oxidation, which corroborates mutually exclusive binding between NH_3 and C_2H_4 at the NH_3-binding site. Whole-cell kinetic studies with AMO in *N. oceanus* (26) showed that Michaelis-Menten kinetics are observed for the physiological substrate NH_3 alone but not when CH_4 is added as an inhibitor of NH_3 oxidation (25, 26). However, no supplemental reductant such as N_2H_4 was added, and so the effects of inhibitor binding to AMO are difficult to separate from the problem of reductant limitation.

The competitive character (defined as $K_{iE} \ll K_{iES}$) of inhibition by CH_4, C_2H_4, C_2H_6, CH_3Cl, and CH_3Br is supported by the optimal N_2H_4 requirements, which decreased with increasing NH_4^+ concentration for a given concentration of inhibitor. The competitive character is further corroborated by Table 4, which shows that oxidation of C_2H_4, CH_3Cl, and CH_3Br decreased at the highest concentrations of NH_4^+. In each case, an optimum NH_4^+ concentration provided maximum oxidation of the alternate substrate, presumably because lower NH_4^+ concentrations provided insufficient reductant whereas supraoptimal concentrations competitively prevented alternate substrate binding to AMO. Our data support not only the findings of Hyman and Wood for CH_4 (13) and C_2H_4 (14) but also the competitive patterns obtained by Suzuki et al. for CH_4, CO, and CH_3OH (23). The curvature observed in the kinetic plots of the previous studies (inhibitor present) (13, 14, 23) disappeared in our plots when the optimal N_2H_4 concentration was added. We thus confirm that reductant depletion in *N. europaea* by oxidation of (competitive) alternate substrates is a primary cause of nonlinear (concave-up) plots, as has been suggested (14). Reductant depletion probably influenced the lower K_{iE} values obtained for CH_4 (2 mM) and C_2H_4 (80 μM) (13, 14). Therefore, only some C_1 and C_2 compounds have been shown to competitively inhibit NH_3 oxidation by AMO.

Binding of noncompetitive inhibitors to the active site may occur at a hydrophobic region, since the inhibitors are all nonpolar. This region is likely to be less well defined than the NH_3-binding site because of the greater structural diversity of alternate substrates that are noncompetitive inhibitors of NH_3 oxidation. Typically, noncompetitive patterns ($K_{iE} \geq K_{iES}$) were associated with a less variable optimal N_2H_4 requirement for a given inhibitor concentration. Since inhibition was not relieved by a high NH_4^+ concentration, NH_3-derived NH_2OH contributed to AMO reduction via HAO in smaller increments as the NH_4^+ concentration increased (relative to competitive inhibition). Also, as shown in Table 4, 40 mM NH_4^+ allowed the greatest production of acetaldehyde from 300 μM C_2H_5Br (0.50 μmol · min^{-1} · mg of $protein^{-1}$). Apparently, some noncompetitive substrates can be oxidized at a site other than the NH_3-binding site and at comparable rates. Rasche et al. found that C_2H_5Cl oxidation rates were undiminished or slightly increased at 40 mM NH_4^+ relative to lower NH_4^+ concentrations over a range of C_2H_5Cl concentrations (19). This result supports noncompetitive binding and oxidation for C_2H_5Cl.

The similarity of V_{max} values for C_2H_4, C_2H_6, and NH_3 is remarkable given that the oxidized bonds (or electron pair) differ in each case. The most plausible explanation is that a common rate-determining step limits oxidation rates for these substrates. It has been suggested that AMO reduction is rate determining in vivo (14). The similar V_{max} values indicate that C_2H_4 and C_2H_6 bind at the active site in an orientation allowing efficient turnover. In contrast, C_2H_5I was a poor substrate relative to other haloethanes but had high affinity for AMO (19). Apparently, C_2H_5I binds in an orientation which does not promote efficient catalysis, as well as inhibiting NH_3 oxidation. How C_2H_4, C_2H_6, and NH_3 might bind to a common site is unknown, but it is interesting that lone electron pairs (NH_3), pi electrons (C_2H_4), and even C—H bonds (C_2H_6) may serve as metal ligands (5).

The inhibitors we chose allowed us to consider several series of structurally related compounds. The first trend in our data was an increase in the K_{iE}/K_{iES} ratio with increasing molecular size. This was observed for the alkane series ($CH_4 < C_2H_6 < C_3H_8 \approx n\text{-}C_4H_{10}$) and for halogenated hydrocarbons with increasingly longer alkyl chains but an identical halogen atom (e.g., CH_3Cl, C_2H_5Cl, $n\text{-}ClC_3H_7$). This pattern also occurred for halomethanes (Cl, Br, I) as a group and also for haloethanes (Cl, Br, I) (halogen radii increase in the order Cl < Br < I). This effect may have arisen from the increasing affinity of larger (and more hydrophobic) inhibitors to an alternate binding site. Also, larger inhibitors might cause greater steric hindrance of proper positioning of the active site (22).

The second trend involved the identity of the halogen substituent on monohalogenated hydrocarbons. The K_{iE}, K_{iES}, and $[\mu M\ I]_{50\%}$ values in Table 2 indicate that chlorinated compounds were generally less effective inhibitors than brominated compounds. The iodinated compounds were the most inhibitory of the monohalocarbons. This trend may have been related to increasing size or nucleophilicity of the halogen atoms (both orders were Cl < Br < I). These data reflect the finding that haloethane reactivity (measured as acetaldehyde production in the presence of NH_3) decreased in the order $C_2H_5Cl > C_2H_5Br > C_2H_5I$ (19).

Another observation was that concave-down reciprocal plots were obtained only for tetrachlorinated compounds. The multiple lone electron pairs on these compounds may

constitute potential ligands that could allow some competition with NH_3 binding to the active site, whereas the molecular size of the compounds would predict a high K_{iE}/K_{iES} ratio. This would explain the concave-down curvature: a disproportionate increase in NO_2^- production rates with increasing NH_4^+ concentration.

Our data support a model in which (i) the NH_3-binding site can be occupied significantly only by C_1 compounds and C_2 hydrocarbons (including C_2H_2 [15]); (ii) iodinated compounds, C_2 (and larger) halogenated compounds, and most hydrocarbons ($>C_2$) would bind predominantly at a more hydrophobic site, to which NH_3 would not bind; and (iii) oxidation of an organic substrate at the alternate site could occur at a rate comparable to oxidation at the NH_3-binding site. Binding at the alternate site could interfere with oxidation at the NH_3-binding site by competing for activated O_2 (i.e., alternate substrate oxidation) or by interfering with turnover (e.g., by drawing the enzyme into a dead-end complex).

Vannelli et al. (24) proposed a model in which an alternate substrate such as *trans*-2-butene was bound to AMO through interactions at two sites. This model, which proposes a single oxidation site, was presented to explain the product ratios (alcohol/epoxide) for the substrates *cis*- and *trans*-2-butene (11) and the relative reactivities of *cis*- and *trans*-dibromoethylene (24). It should be noted that differing bond dissociation energies and the intrinsic steric inaccessibility of the pi bonds may have accounted for the product ratios (11, 24). Our model and the model of Vannelli et al. are not necessarily mutually exclusive; substrate binding orientations are not excluded by our model as a factor influencing bond reactivities, product ratios, or inhibition patterns.

Our model describes the experimental results in terms of the direct interactions of the inhibitors with AMO. However, given that the experiments were carried out with intact cells, other factors may have influenced the results. For example, the inhibitors could have altered the activities of enzymes other than AMO that are required for the coupled assay. This appeared not to be the case, given that the oxidation of NH_2OH was not substantially altered by the inhibitors. If an NH_4^+/NH_3 diffusion gradient existed across the periplasmic membrane, addition of inhibitors could alter this gradient. Decreasing the activity of AMO would be expected to cause a shallowing of any diffusion gradient and a decrease in the apparent K_m for NH_4^+ (17). However, specific inactivation of AMO by light resulted in only small changes in the apparent K_m for NH_4^+, which suggests that the diffusion gradient, if it existed, was small. Therefore, if the AMO inhibitors we used also diminished the apparently small gradient, only small decreases in curve slopes on the double-reciprocal plots would have resulted. It is also possible that AMO is part of a multienzyme complex in intact cells and that the kinetics we have measured are a reflection of the complex rather than the active site of AMO. Because of these and additional factors that could influence the values of measured kinetic constants, the values are referred to as apparent kinetic constants to distinguish them from the constants that would be determined if active, purified enzyme preparations were available.

In our experiments, N_2H_4 was added as a source of reductant, so that reductant limitation was not a factor influencing the observed kinetics. The results provide a basis for predicting the outcome when N_2H_4 is not included and NH_4^+ is the only source of reductant. For noncompetitive inhibitors ($K_{iE} > K_{iES}$) which are also substrates, the rate of oxidation of the alternate substrate should not decrease substantially at high NH_4^+ concentrations (>20 mM). In contrast, for the alternate substrates that are competitive inhibitors of NH_3 oxidation or display competitive character ($K_{iE} \ll K_{iES}$), their rate of oxidation should decrease substantially at high NH_4^+ concentrations. In both cases, low concentrations of alternate substrates will inhibit AMO activity by depleting the NH_3-derived reductant supply. The predicted results were observed for a competitive inhibitor (C_2H_4), a distinctly noncompetitive inhibitor (C_2H_5Br), and two noncompetitive inhibitors with competitive character (CH_3Cl and CH_3Br) (Table 4).

In summary, we have observed trends regarding hydrocarbon and halogenated hydrocarbon inhibition of NO_2^- production by whole cells of *N. europaea*. The trends reflect structural relationships of the inhibitors: increasing molecular size produced increasing K_{iE}/K_{iES} ratios, and increasing halogen size was correlated with greater inhibitor effectiveness. Corroborating studies indicated that high NH_3 concentrations decreased oxidation rates for alternate substrates with competitive character ($K_{iE} \ll K_{iES}$) as inhibitors of NO_2^- production but not for substrates with predominantly noncompetitive character ($K_{iE} \geq K_{iES}$). These results support an active-site model for AMO consisting of (at least) two substrate-binding sites in addition to the O_2-binding site and the site of electron donation to AMO; oxidation may occur at either site. The correlation of structural relationships with the observed trends indicates that our data should allow predictions for structurally related compounds regarding their interactions with NH_3 at the active site of AMO.

ACKNOWLEDGMENTS

This research was supported by U.S. Environmental Protection Agency grant R816531 and the Oregon Agricultural Experiment Station.

We gratefully acknowledge Michael Hyman, Scott Ensign, and Luis Sayavedra-Soto for providing helpful comments and suggestions.

REFERENCES

1. **Anderson, J. H.** 1965. Studies on the oxidation of ammonia by *Nitrosomonas*. Biochem. J. **95**:688–698.
2. **Arciero, D. M., T. Vannelli, M. Logan, and A. B. Hooper.** 1989. Degradation of trichloroethylene by the ammonia-oxidizing bacterium *Nitrosomonas europaea*. Biochem. Biophys. Res. Commun. **159**:640–643.
3. **Bédard, C., and R. Knowles.** 1989. Physiology, biochemistry, and specific inhibitors of CH_4, NH_4^+, and CO oxidation by methanotrophs and nitrifiers. Microbiol. Rev. **53**:68–84.
4. **Cornish-Bowden, A.** 1979. Inhibitors and activators, p. 73–98. *In* Fundamentals of enzyme kinetics. Butterworths, Boston, Mass.
5. **Crabtree, R. H., and D. G. Hamilton.** 1988. H-H, C-H, and related sigma-bonded groups as ligands, p. 299–338. *In* F. G. Stone, and R. West (ed.), Advances in organometallic chemistry. Academic Press, Inc., San Diego, Calif.
6. **Ensign, S. A., M. R. Hyman, and D. J. Arp.** 1993. In vitro activation of ammonia monooxygenase from *Nitrosomonas europaea* by copper. J. Bacteriol. **175**:1971–1980.
7. **Gornall, A. G., C. J. Bardawill, and M. M. David.** 1949. Determination of serum proteins by means of the biuret reaction. J. Biol. Chem. **177**:751–766.
8. **Hageman, R. H., and D. P. Hucklesby.** 1971. Nitrate reductase from higher plants. Methods Enzymol. **23**:491–503.
9. **Hyman, M. R.** 1985. Ph.D. thesis. University of Bristol, Bristol, United Kingdom.
10. **Hyman, M. R., and D. J. Arp.** 1992. $^{14}C_2H_2$- and $^{14}CO_2$-labelling studies of the *de novo* synthesis of polypeptides by *Nitrosomonas europaea* during recovery from acetylene and light inacti-

vation of ammonia monooxygenase. J. Biol. Chem. **267**:1534–1545.
11. **Hyman, M. R., I. B. Murton, and D. J. Arp.** 1988. Interaction of ammonia monooxygenase from *Nitrosomonas europaea* with alkanes, alkenes, and alkynes. Appl. Environ. Microbiol. **54**: 3187–3190.
12. **Hyman, M. R., A. W. Sansome-Smith, J. H. Shears, and P. M. Wood.** 1985. A kinetic study of benzene oxidation to phenol by whole cells of *Nitrosomonas europaea* and evidence for the further oxidation of phenol to hydroquinone. Arch. Microbiol. **143**:302–306.
13. **Hyman, M. R., and P. M. Wood.** 1983. Methane oxidation by *Nitrosomonas europaea*. Biochem. J. **212**:31–37.
14. **Hyman, M. R., and P. M. Wood.** 1984. Ethylene oxidation by *Nitrosomonas europaea*. Arch. Microbiol. **137**:155–158.
15. **Hyman, M. R., and P. M. Wood.** 1985. Suicidal inactivation and labelling of ammonia monooxygenase by acetylene. Biochem. J. **227**:719–725.
16. **Lees, H.** 1952. The biochemistry of the nitrifying organisms. 1. The ammonia-oxidizing systems of *Nitrosomonas*. Biochem. J. **52**:134–139.
17. **Martinez, M. B., F. J. Schendel, M. C. Flickinger, and G. L. Nelsestuen.** 1992. Kinetic properties of enzyme populations *in vivo*: alkaline phosphatase of the *Escherichia coli* periplasm. Biochemistry **31**:11500–11509.
18. **Nicholas, D. J., and O. T. G. Jones.** 1960. Oxidation of hydroxylamine in cell-free extracts of *Nitrosomonas europaea*. Nature (London) **185**:512–514.
19. **Rasche, M. E., R. E. Hicks, M. R. Hyman, and D. J. Arp.** 1990. Oxidation of monohalogenated ethanes and *n*-chlorinated alkanes by whole cells of *Nitrosomonas europaea*. J. Bacteriol. **172**:5368–5373.
20. **Rasche, M. E., M. R. Hyman, and D. J. Arp.** 1990. Biodegradation of halogenated hydrocarbon fumigants by nitrifying bacteria. Appl. Environ. Microbiol. **56**:2568–2571.
21. **Rasche, M. E., M. R. Hyman, and D. J. Arp.** 1991. Factors limiting aliphatic chlorocarbon degradation by *Nitrosomonas europaea*: cometabolic inactivation of ammonia monooxygenase and substrate specificity. Appl. Environ. Microbiol. **57**: 2986–2994.
22. **Segel, I. H.** 1976. Enzymes, p. 208–323. *In* Biochemical calculations. John Wiley & Sons, Inc., New York.
23. **Suzuki, I., S.-C. Kwoks, and U. Dular.** 1976. Competitive inhibition of ammonia oxidation in *Nitrosomonas europaea* by methane, carbon monoxide, or methanol. FEBS Lett. **72**:117–120.
24. **Vannelli, T., M. Logan, D. M. Arciero, and A. B. Hooper.** 1990. Degradation of halogenated aliphatic compounds by the ammonia-oxidizing bacterium *Nitrosomonas europaea*. Appl. Environ. Microbiol. **56**:1169–1171.
25. **Ward, B. B.** 1987. Kinetic studies on ammonia and methane oxidation by *Nitrosococcus oceanus*. Arch. Microbiol. **147**:126–133.
26. **Ward, B. B.** 1990. Kinetics of ammonia oxidation by a marine nitrifying bacterium: methane as a substrate analogue. Microb. Ecol. **19**:211–225.
27. **Weatherburn, M. W.** 1967. Phenol-hypochlorite reaction for determination of ammonia. Anal. Chem. **39**:971–974.
28. **Wood, P. M.** 1986. Nitrification as a bacterial energy source, p. 39–62. *In* J. I. Prosser (ed.), Nitrification. Society for General Microbiology (IRL Press), Washington, D.C.